Supporting Information

Latrunculin Analogues with Improved Biological Profiles by "Diverted Total Synthesis": Preparation, Evaluation and Computational Analysis

Alois Fürstner,* Douglas Kirk, Michaël D. B. Fenster, Christoph Aïssa, Dominic De Souza, Laurent Turet, Christina Nevado, Tell Tuttle, Walter Thiel, and Oliver Müller[‡]

Max-Planck-Institut für Kohlenforschung, D-45470 Mülheim/Ruhr (Germany)
Email: fuerstner@mpi-muelheim.mpg.de

[‡]*Max-Planck-Institut für Molekulare Physiologie, D-44227 Dortmund (Germany)*

1. Computational Methods

Structure preparation: The structure of G-actin with latrunculin A (**1**) bound is available from the protein data bank (PDB ID: 1ESV).[1] There are several completely unresolved residues in the protein structure, although as these residues are remote from the binding site, the backbone was capped with neutral residues at these positions. The protonation state of the ionizable residues was checked with PROPKA[2] and REDUCE,[3,4] which was also used to determine the orientation of the ambiguous residues (HIS, ASN, GLN). The crystal waters, three Ca^{2+} ions and ATP were retained, however no additional hydration was performed.

A conformational search was performed for **1** and two of its analogs (Latrunculin B (**2**) and the fully synthetic compound **44**) using the PM3 Hamiltonian as implemented in Spartan.[5] The ten lowest energy conformers of each molecule were selected and subsequently optimized within MNDO99[6] using the MNDO/H Hamiltonian,[7,8] which provides reasonable geometries and relative energies for hydrogen bonded systems.[7,9] The reliability of the semi-empirical structures was checked via re-optimization of the conformers at the BLYP[10,11] level of theory with the def2-SVP basis set[12] available in TURBOMOLE.[13-17]

Docking: For each compound, the ten conformers (optimized with BLYP) were then docked into the actin binding site using AUTODOCK 3.0 (AD3).[18] The AD3 grid was constructed such that it encompassed and was centered on the binding site of **1** (available from the original PDB). AD3 is not parameterized for substrates, such as ATP or Ca^{2+} and as such these residues are ignored during the docking procedure. As ten different conformational variants of each ligand were tested, the ligand was kept rigid during the

docking process. The orientation resulting in the best binding energy for each conformer was selected from each docking run for optimization.

Force field minimization: The complex with the best binding energy from each docking simulation was pre-minimized in CHARMM.[19-21] The standard CHARMM force field[22-24] used in this work does not contain parameters for the **1**, **2** or **44**. However, given the preparative nature of the force field minimization, the parameters and topology of the ligands were automatically generated using the commercial CHARMm force field[25] in the Accelrys suite of programs. The ligands were kept rigid and the remainder of the system was then relaxed during a 10,000-step ABNR minimization.

QM/MM optimization: The structures resulting from the force field minimization were optimized at the hybrid quantum mechanical/molecular mechanical (QM/MM) level of theory with the modular program package CHEMSHELL.[26,27] The QM energy and gradients were provided by MNDO99,[6] with MNDO/H[7,8] as the QM level of theory. CHEMSHELL's internal forcefield driver, using the CHARMM parameter and topology data[22-24] supplied the MM energy and gradients. No electrostatic cut-offs were employed in the QM/MM calculations. Electrostatic embedding[28] with the charge-shift scheme[27,29] was used to couple the QM and MM regions.

The QM/MM geometry optimizations were performed with the HDLCOpt algorithm,[30] as implemented in CHEMSHELL. The QM region was defined to include all atoms of the ligand, whereas the receptor, counterions and ATP were contained in the MM region. A subset of the total system (the active region) is optimized in the QM/MM procedure. The active region is defined from the starting geometry – any residue that contains an atom within 20.0 Å of the ligand is included in the active subset. The resulting active region

contains ca. 4100 atoms, which is slightly less than half of the total system size (ca. 9000 atoms).

Homodesmotic reactions: The results from independent optimizations of the complexes can not be compared directly, in terms of absolute energies, due to the distance criteria used in the determination of the active atoms during each optimization. That is, the number and type of the atoms optimized in each complex varies, which implies that the results are no longer fully compatible. Thus, in order to calculate the relative binding energies ($??E_{bind}$) from the homodesmotic reactions the **2**/G-actin and **44**/G-actin complexes were optimized using the optimized **1**/G-actin complex as a starting point. The **2**/G-actin and **44**/G-actin complexes were created by subsequently deleting the additional groups (i.e. for **2** the HC=CH linkage in the macrocycle was deleted, then the methyl substituents were deleted to create the **44** complex). After this initial preparation, the complexes were optimized using a smaller distance criterion (10 Å) for the active region. The smaller optimization region and the common starting point ensured all systems were optimized to an equivalent state.

2. Conformational Search Results

The original ordering was obtained from the conformational search performed in SPARTAN using the PM3 Hamiltonian. The structures resulting from this search were re-optimized at the MNDO/H level of theory and subsequently at the RI-BLYP/def2-SVP level. The ordering of the conformers changes as a result of these optimizations. Table S1 lists the relative energies (kcal/mol) of the BLYP-optimized structures that were used in the subsequent docking studies.

Table S1. BLYP relative energies (kcal/mol).[a]

Original	1	2	44
1	0.00	0.00	0.00
2	0.22	3.30	0.07
3	0.41	7.00	0.66
4	2.92	6.39	-2.35
5	-1.91	-0.07	-2.33
6	1.29	3.96	0.73
7	-2.20	2.70	0.71
8	2.38	3.42	-2.08
9	-2.00	7.60	1.66
10	2.00	6.74	0.13

[a]Relative to the lowest-energy PM3 conformer (no. 1).

3. Docking Simulation and QM/MM Optimization of Complexes

Only the best-docked structure (min ΔE_b) is given. Qualitatively the orientation of the substrate in the binding site has been compared to that of the crystal structure. Those structures with a good general agreement with the crystal structure are listed as "Yes" in the "Overlap" column of Tables S4-S6. The conformer number refers to the original ordering defined in Table S1.

Table S2. Docking simulation results and subsequent QM/MM optimizations for conformers of **1**.[a]

Conf #	ΔE_b	Overlap	ΔE_{QM}	ΔE_{MM}	$\Delta E_{QM/MM}$
1	-8.90	Yes	0.00	0.00	0.00
2	-9.67	No	30.35	47.85	78.21
3	-10.00	Yes	22.42	-56.82	-34.40
4	-9.32	No	93.63	204.57	298.20
5	-9.28	No	27.20	29.88	57.09
6	-9.40	No	25.26	122.95	148.20
7	-11.58	Yes	11.58	-55.30	-43.72
8	-10.30	Yes	7.52	-27.48	-19.96
9	-11.17	Yes	8.56	-34.77	-26.21
10	-7.72	No	26.67	-3.83	22.84

[a]Conf #: the conformer ordering obtained from the original search. ΔE_b: the binding energy calculated by AUTODOCK. Overlap: whether the docked structure is similar to the crystal structure. ΔE_{QM}: the QM energy of the structure, relative to the QM energy of the least stable conformer with an orientation similar to the crystal structure. ΔE_{MM}: the MM energy of the structure, relative to the MM energy of the least stable conformer with an orientation similar to the crystal structure. $\Delta E_{QM/MM}$: the QM/MM energy of the structure, relative to the QM/MM energy of the least stable conformer with an orientation similar to the crystal structure. All energies are in kcal/mol.

All of the orientations obtained in the docking study of **1** could be optimized at the QM/MM level. The AD3 energies (ΔE_b, Table S2) are all stabilizing and indicate

reasonably strong binding (binding energies between -7 and -12 kcal/mol). However, the AD3 results should be viewed with much caution because AD3 does not account for the presence of ATP or Ca^{2+} ions. It is thus not surprising that the more reliable QM/MM optimization results differ strongly. The QM/MM data shows a clear preference for the orientation observed in the crystal structure (Overlap = Yes, Table S2). All other structures, whose orientation differs strongly from the crystal structure are strongly destabilized ($\Delta E_{QM/MM}$, Table S2). The relative QM/MM energies indicate that the most stable complex is obtained from conformer 7. The corresponding QM/MM structure was used in all subsequent studies of the **1**/G-actin complex.

Table S3. Docking simulation results and subsequent QM/MM optimizations for conformers of **2**.

Conf #	ΔE_b	Overlap	ΔE_{QM}	ΔE_{MM}	$\Delta E_{QM/MM}$
1	-9.40	No	26.10	38.16	64.26
2	-9.12	No	17.33	8.18	25.52
3	-10.27	Yes	0.00	0.00	0.00
4	-9.95	No	45.78	139.85	185.63
5	-10.92	Yes	7.50	-28.81	-21.31
6	-8.85	No	114.14	160.37	274.51
7	-9.06	No	13.16	13.68	26.84
8	-9.46	No	168.61	200.52	369.13
9	-9.72	No	52.05	236.41	288.46
10	-9.77	No	—	—	—

[a]See footnote of Table S2 for details.

All orientations, except conformer 10, obtained in the docking study of **2** could be optimized at the QM/MM level. The AD3 energies are stabilizing and are even more closely clustered than in the docking study of **1**. Again the QM/MM optimization reveals much greater differences between the structures than the AD3 results. Of the nine optimized structures, only two of these have an orientation similar to the crystal structure. As in the case of **1**, these two systems are clearly the most favorable. The lowest-energy complex resulted from the docking study with conformer 5, thus this structure was used for further analysis.

Table S4. Docking simulation results and subsequent QM/MM optimizations for conformers of **44**.

| Conf #	$?E_b$	Overlap	$?E_{QM}$	$?E_{MM}$	$?E_{QM/MM}$
1	-9.24	No	15.17	240.75	255.92
2	-10.14	No	—	—	—
3	-9.45	No	—	—	—
4	-8.71	No	—	—	—
5	-9.35	No	—	—	—
6	-9.01	Yes	0.00	0.00	0.00
7	-8.97	No	13.70	170.54	184.24
8	-8.25	No	—	—	—
9	-8.70	No	21.40	229.13	250.52
10	-9.55	No	277.55	283.70	561.25

[a]See footnote of Table S2 for details.

The fact that the ATP ligand was missing during the docking study had severe consequences in the docking of compound **44**. The smaller ring size of **44** allowed it to adopt a greater range of positions, which generally involved placing the macrocycle deeply into the hydrophobic pocket. However, this often led to an overlap with the ATP residue and as such the structures could not be optimized. In the case of smaller overlap the optimizer was able to correct the structure, at the expense of strongly destabilizing MM contributions (Table S4). One simulation resulted in a structure close to the natural **1** position (conformer 6) and the subsequent QM/MM optimization confirmed that this structure was significantly more stable than the others. It was therefore selected to represent the **44**/G-actin complex.

4. Hydrophobic Contributions.

The contribution from the hydrophobic effect will aid in stabilizing the ligands in the binding site. In Figure S1, the hydrophobicity of the binding pocket in the **1**/G-actin complex is mapped onto a Connolly surface[31,32] of the receptor. The hydrophobicity is determined by the partial charges on the residues (assigned in the CHARMM force field). The majority of the macrocycle prefers a hydrophobic environment (green regions in Figure S1). This is achieved by a small part of the macrocycle (lower left region in Figure S1), although the majority of the system is solvent exposed (no surface) or surrounded by polar (red) residues.

Figure S1. Hydrophobicity mapped onto a Connolly surface of the receptor in the **1**/G-actin complex.
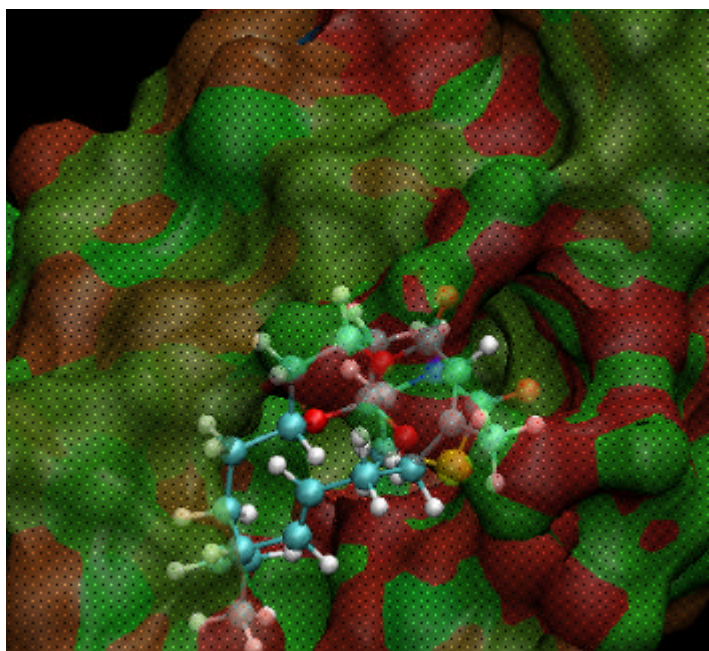
The hydrophobic contribution to the stability of the complex may be estimated using an empirical function based on the change in the solvent accessible surface area (?SASA) in the bound and unbound states. The relationship proposed by Spolar and Record:[33]

$$\Delta G_{hyd} = -22(\pm 5)\, \Delta SASA \qquad (1)$$

results in a stabilizing free energy contribution of -20 ± 4.5 kcal/mol when the **1**/G-actin complex is formed. For the smaller ligands **2** and **44** the stabilizing effect is slightly smaller (-19 ± 4.3 kcal/mol and -17 ± 4.3 kcal/mol) as a greater percentage of the ligand remains solvent exposed in the optimized structures. The calculated values clearly indicate that the binding of the ligand is favorable from a hydrophobic perspective, however, given that the error bars for this calculation overlap in all cases, the criterion offers no clear distinction between the three ligands.

References

(1)   Morton, W. M.; Ayscough, K. R.; McLaughlin, P. J. *Nature Cell Biol.* **2000**, *2*, 376.

(2)   Li, H.; Robertson, A. D.; Jensen, J. H. *Proteins: Struct. Func.* **2005**, *61*, 704.

(3)   Word, J. M. *Reduce*, V. 2.21; Durham, NC, 2003

(4)   Word, J. M.; Lovell, S. C.; Richardson, J. S.; Richardson, D. C. *J. Mol. Biol.* **1999**, *285*, 1735.

(5)   *Spartan*, V. 5.1, Wavefunction, Inc.; Irvine, CA.

(6)   Thiel, W. *MNDO99*, V. 6.1; Max-Planck-Institut für Kohlenforschung: Mülheim an der Ruhr, Germany, 2004

(7)   Burstein, K. Y.; Isaev, A. N. *Theor. Chim. Acta.* **1984**, *64*, 397.

(8)   Dewar, M. J. S.; Thiel, W. *J. Am. Chem. Soc.* **1977**, *99*, 4899.

(9)   Goldblum, A. *J. Comp. Chem.* **1987**, *8*, 835.

(10) Becke, A. D. *Phys. Rev. A* **1988**, *38*, 3098.

(11) Lee, C. T.; Yang, W. T.; Parr, R. G. *Phys. Rev. B* **1988**, *37*, 785.

(12) Weigend, F.; Ahlrichs, R. *Phys. Chem. Chem. Phys.* **2005**, *7*, 3297.

(13) *TURBOMOLE*, V. 5.7.1, 2004

(14) Ahlrichs, R.; Bär, M.; Häser, M.; Horn, H.; Kölmel, C. *Chem. Phys. Lett.* **1989**, *162*, 165.

(15) Häser, M.; Ahlrichs, R. *J. Comp. Chem.* **1989**, *10*, 104.

(16) Horn, H.; Weiss, H.; Häser, M.; Ehrig, M.; Ahlrichs, R. *J. Comp. Chem.* **1991**, *12*, 1058.

(17) Treutler, O.; Ahlrichs, R. *J. Chem. Phys.* **1995**, *102*, 346.

(18) Morris, G. M.; Goodsell, D. S.; Halliday, R. S.; Huey, R.; Hart, W. E.; Belew, R. K.; Olson, A. J. *J. Comp. Chem.* **1998**, *19*, 1639.

(19) *CHARMM*, V. c31b1, 2004

(20) Brooks, C. L.; Karplus, M. *J. Chem. Phys.* **1983**, *79*, 6312.

(21) MacKerell, A. D.; Brooks, B. R.; Brooks, C. L., III; Nilsson, L.; Roux, B.; Won, Y.; Karplus, M. In *Encyclopedia of Computational Chemistry*; Schleyer, P. v. R., Ed.; Wiley: Chichester, 1998; Vol. 1, p 271.

(22) Foloppe, N.; MacKerell, A. D. *J. Comp. Chem.* **2000**, *21*, 86.

(23) MacKerell, A. D.; Banavali, N. K. *J. Comp. Chem.* **2000**, *21*, 105.

(24) MacKerell, A. D. *et. al. J. Phys. Chem. B* **1998**, *102*, 3586.

(25) The commercial and academic versions of the CHARMM force fields are not strictly compatible. However, the parameters for the non-bonding terms (van der Waals and Coulombic interactions) are comparable.

(26) *ChemShell*, V. 3.0a3, 2004

(27) Sherwood, P. *et. al. J. Mol. Struct. (Theochem)* **2003**, *632*, 1.

(28) Bakowies, D.; Thiel, W. *J. Phys. Chem.* **1996**, *100*, 10580.

(29) de Vries, A. H.; Sherwood, P.; Collins, S. J.; Rigby, A. M.; Rigutto, M.; Kramer, G. J. *J. Phys. Chem. B* **1999**, *103*, 6133.

(30) Billeter, S. R.; Turner, A. J.; Thiel, W. *Phys. Chem. Chem. Phys.* **2000**, *2*, 2177.

(31) Connolly, M. L. *J. App. Cryst.* **1983**, *16*, 548.

(32) Connolly, M. L. *Science* **1983**, *221*, 709.

(33) Spolar, R. S.; Record, M. T. *Science* **1994**, *263*, 777.